# Image Contrast in the Lateral Force Mode in Multiphase Nanomaterials

O.V.Carban, E.I.Salamatov, S.G.Bystrov, A.V.Zhikharev

*Physico-Technical Institute UrB of RAS,*
*132 Kirov st., Izhevsk, 426001 Russia*

*(Received 26 February 2001, accepted for publication 1 March 2001)*

Peculiarities of the image contrast formation have been studied while investigating samples with different surface topography by lateral force microscopy (LFM). The main contribution to the lateral image contrast has been shown to come from the chemical composition, which makes it possible to use this method for distinguishing between structurally close nanophases. The contrast formation has been analyzed at various scan rates.

## Introduction

It is well known [1] that many properties of nanomaterials (elastic, thermal and dielectric) are determined by the crystallite size and the interface structure depending on the preparation technology. That is why of great importance is the study of the material structure at micro- and nanoscales. Conventional methods for the material structure investigation like X-ray diffraction, SEM and TEM are not always suitable for this purpose. The atomic force microscopy (AFM) intensively developed in the last years allows one to determine the peculiarities of the nanomaterial topography at the cleaved surface which are due to the structural characteristics at the nanoscale. The results of topographical AFM studies may be substantially enhanced by simultaneous analysis of the LFM-images. The measured lateral force is strongly related to the surface physico-chemical properties of the nanoareas. Therefore this method is used to study adhesion, friction, scratching/wear, indentation etc. The main difficulty arising when interpreting the lateral image obtained consists in distinguishing between the contributions to the image contrast coming from the topographical features and the local physico-chemical characteristics of the surface. This problem is especially urgent in the multiphase structure investigation. The present work is devoted to estimation of the effect of the surface roughness and the scan rate

on the lateral-force image contrast of different phases in multiphase materials previously studied by various techniques.

## Specimens and experimental

The measurements were performed using a P4-Solver scanning probe microscope (NT-MTD, Russia) and silicon rectangular cantilevers (CS12, NT-MTD) with the radius of curvature of the tip of less than 10 nm. The scanning direction was perpendicular to the long axis of the cantilever beam. The scan rate ranged from 0.2 to 45 $\mu$m/sec. The samples under investigation were classified into three groups:

a) single crystals of $Y_{1-x}Er_xAlO_3$ ($x = 0.05, 0.07, 0.1, 0.2$) grown by horizontally oriented crystallization;

b) nanoceramics obtained by magnetic-pulse compacting [2] of $Al_2O_3 + 1.5\%$ MgO powder with subsequent baking at various temperatures in the range of 1000–1450°C;

c) the cermet obtained by pressing at room temperature and sintering at 1940 K in vacuum of the $Al_2O_3$ powder and steel powder of the $Fe_{71}Cr_{18}Ni_{10}Ti_1$ composition. The cermet composition was 81% of $Al_2O_3$ and 19% of steel [3].

The samples were freshly cleaved and studied in the air atmosphere.

## Experimental results and discussion

a) Aluminates $Y_{1-x}Er_xAlO_3$

The single crystals of $Y_{1-x}Er_xAlO_3$ are widely used as laser materials. X-ray diffraction studies of the structure of these materials did not reveal the presence of nanoscale areas, whereas the results of the experiments on the concentrational dependence of nuclear magnetic resonance (NMR) spectra provide indirect evidence for the cluster formation and the appearance of nanophases of $Y_{7/8}Er_{1/8}AlO_3$ and $Y_{1/8}Er_{7/8}AlO_3$ composition in these crystals [4]. The difference in the point defect concentration between these nanophases [5] caused by crystallization conditions is responsible for different mechanical characteristics of these nanoareas. For AFM investigation areas with monotonous surface relief were selected. Root mean square roughness ($R_q$) was less than 5 nm. The LFM study of aluminates in lateral force mode revealed the presence of local areas with different physico-chemical properties. Alternating stripes 20–100 nm in width of different brightness constitute the observed structure. An image representative of the structure observed is given in Fig.1 for $Y_{0.8}E_{0.2}AlO_3$.

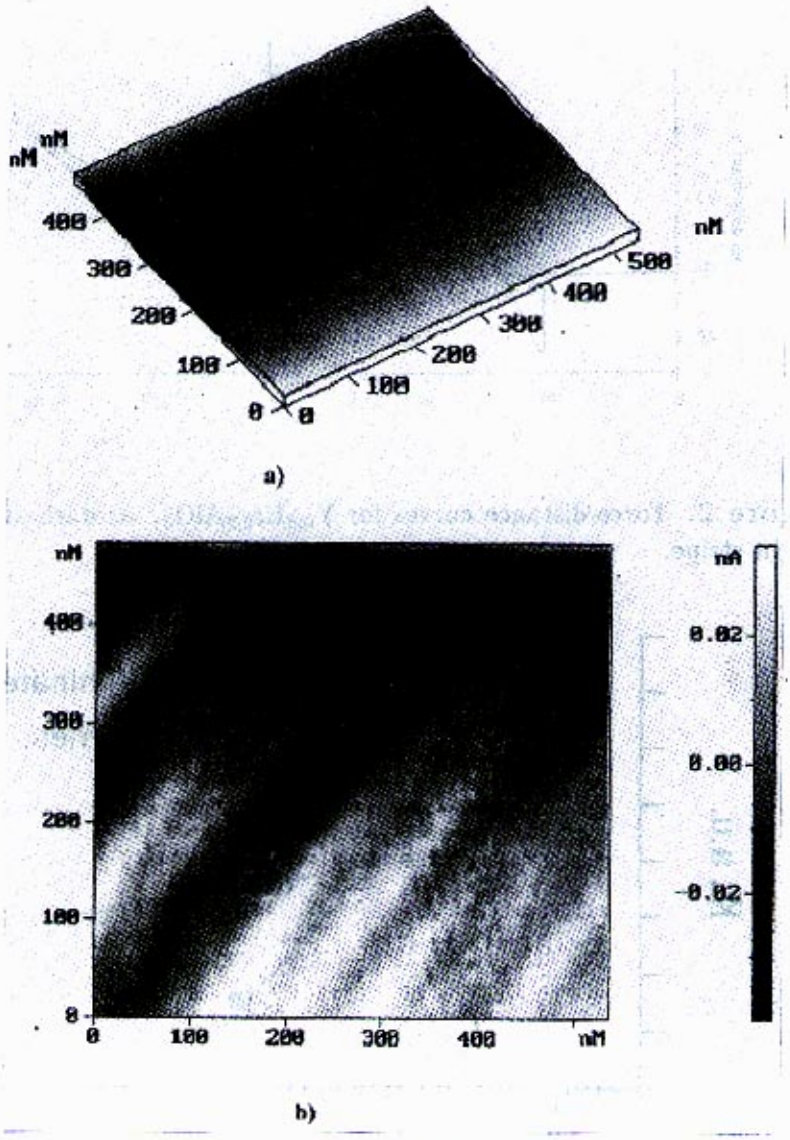


**Figure 1.** 3D-AFM image (a) and 2D-LFM image (b) for $Y_{0.8}Er_{0.2}AlO_3$.

Lower brightness corresponds to smaller lateral friction force. Hardness of the Er-enriched nanoareas is presumably lower than that of the Er-depleted areas, which must result in the increase in the friction force due to a larger tip-sample contact area. Hence, a greater lateral friction force (dark stripe) corresponds to Er-enriched nanoareas. This structure remains unchanged when varying both the scan size and scanning direction. The stripe width depends on the erbium content.

Adhesive force measurements were performed in the "force calibration mode"

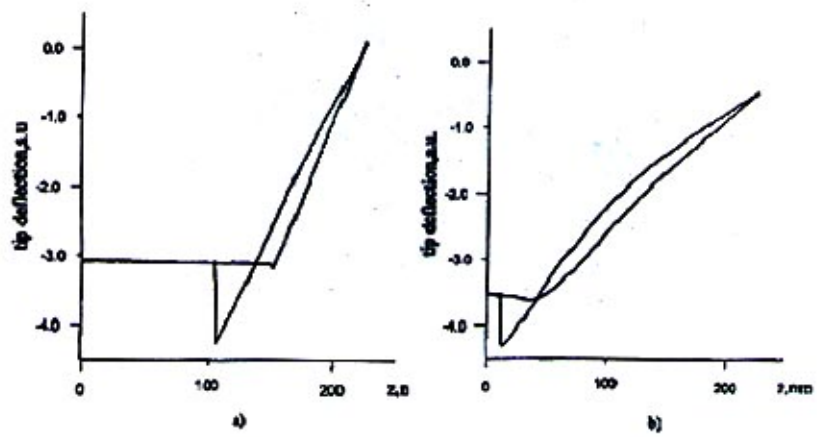

**Figure 2.** Force-distance curves for $Y_{0.8}Er_{0.2}AlO_3$. a) dark stripe; b) bright stripe.

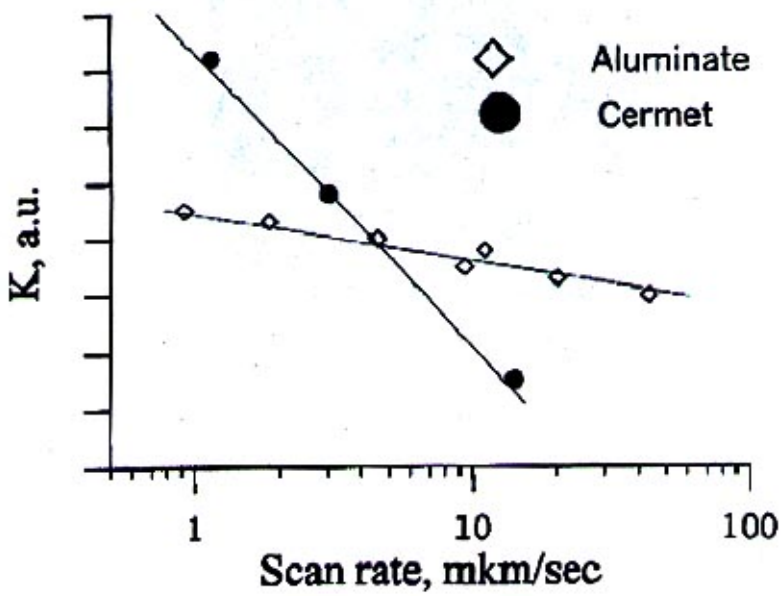


**Figure 3.** Phase contrast $K$ vs the scan rate.

[6]. The adhesive force variation for dark (Fig. 2a) and bright (Fig. 2b) nanoareas may be judged from the force distance curves. As we have used a polar tip (silicon oxide), the increase in the force of tip-surface adhesion suggests an increase in polarity and a decrease in hydrophobic characteristic of the surface. This is due to the fact that the more defect phase (enriched in Er) has a more chemically active surface.

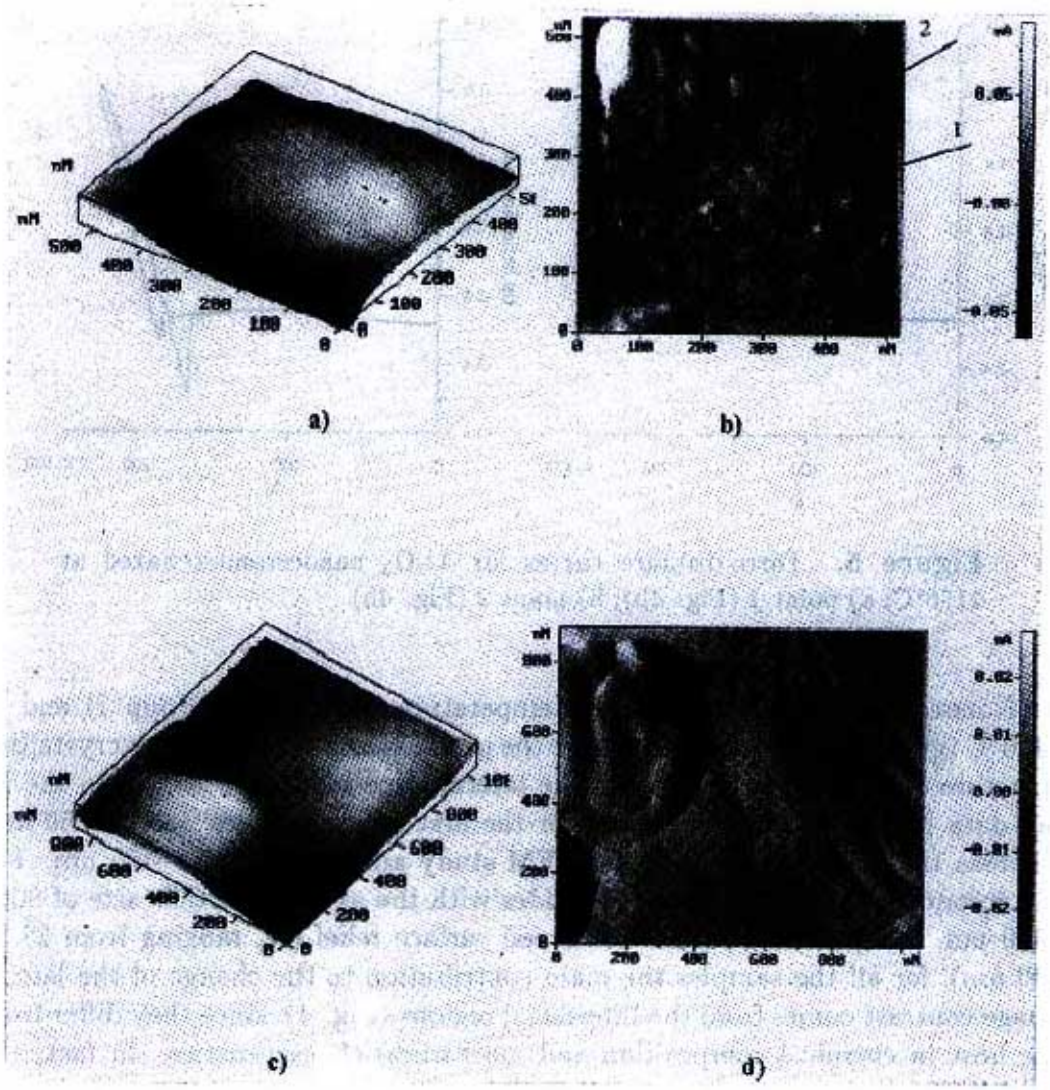


**Figure 4.** 3D-AFM image (a,c) and 2D-LFM image (b,d) for $Al_2O_3$ nanoceramics baked at 1170° (a,b) and at 1410°C (c,d).

Dependence of the lateral force on the scan rate was investigated for the scan rates ranging from 0.9 to 45 $\mu$m/s. Fig. 3 shows the scan-rate dependence of the phase contrast $K$ which was defined as the normalized difference between the maximum and minimum values of the friction coefficient for the given sample. With decreasing scan rate the phase contrast increases (Fig. 3), which is in agreement with previous results [7].

b) $Al_2O_3$ nanoceramic

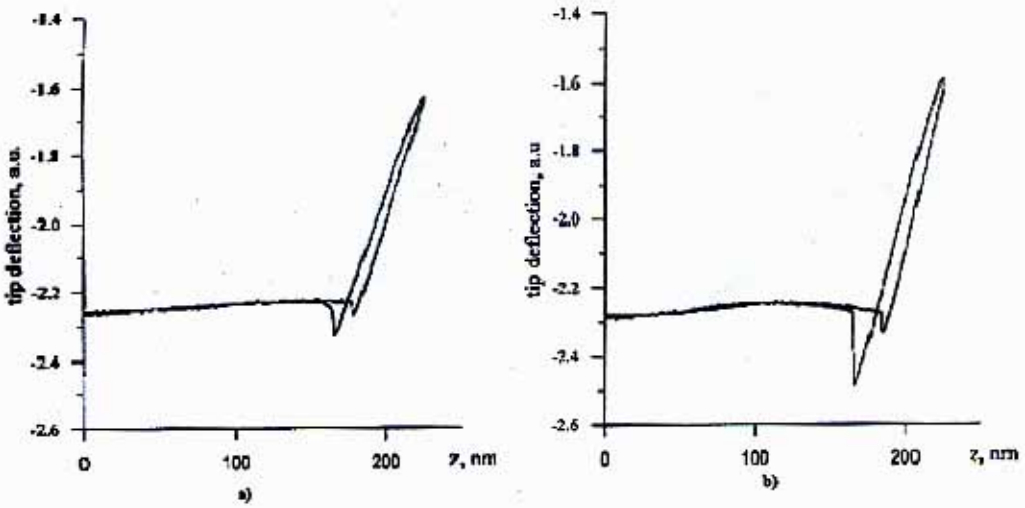


**Figure 5.** Force-distance curves for $Al_2O_3$ nanoceramics baked at 1170°C: a) point 1 (Fig. 4b); b) point 2 (Fig. 4b).

Nanoceramic samples baked at temperatures < 1300°C (group I) and > 1400°C (group II) were chosen to solve the problem of the effect of polycrystalline structure on the image contrast in the lateral force mode. According to the X-ray data [2], the average grain size for the first-group samples was 25–150 nm, whereas the particle size from the AFM study amounted to 200–450 nm. For the second group the grain size coincides with the average particle size of 800–1500 nm. In spite of a rather developed surface relief ($R_q$ ranging from 25 to 130 nm), for all the samples the main contribution to the change of the lateral image contrast comes from the interfacial regions (Fig. 4), since they differ from the host in chemical composition and mechanical characteristics. In fact, the adhesive forces between tip and sample differ (Fig. 5) for the surface areas at the interface (point 2) and beyond it (point 1 in Fig. 4b). Since the AFM-images for the samples of the first group exhibit no difference in contrast between the grains, it may be concluded that the difference in grain orientation does not affect the lateral force image contrast.

The lateral image allows one to obtain additional information on the surface relief and the structure of the interfacial regions. In the first group of samples breakdown occurs by the intercrystallite mechanism, for the second group the nature of breakdown changes from intercrystalline to intercrystallite. A structure of 25–35 nm size detected in the lateral force mode for the second group samples is likely to correspond to the regions of stress concentration emerging during secondary recrystallization of the samples. The size of the detected

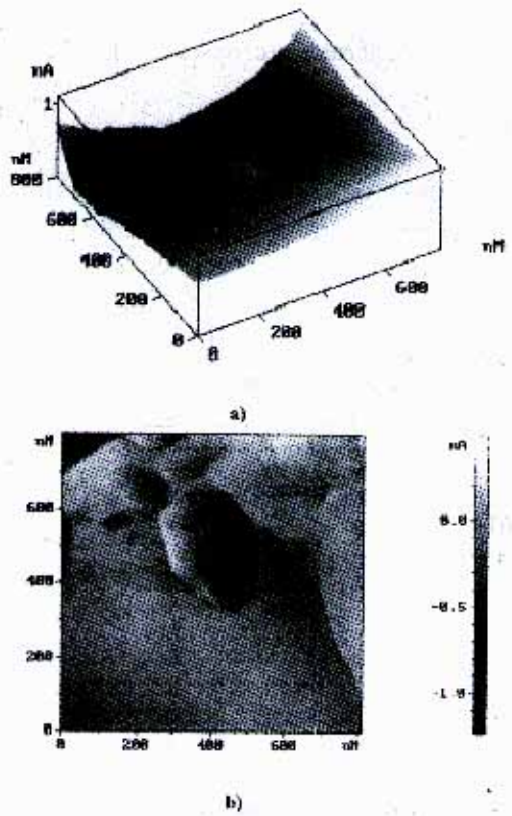


**Figure 6.** 3D-AFM image (a) and 2D-LFM image (b) for cermet.

structure is similar to the grain size of the original powder.

c) Cermet

The metal-ceramic materials (cermets) on the basis of metal oxides ($Al_2O_3$) sintered together with metal powder exhibit extreme strength and chemical and heat resistance. The scanning electron microscopy made it possible to estimate the size of structural elements of these cermets but did not succeed in determining the shape of Fe particles and in distinguishing between embedded particles and pores [3]. The AFM investigation showed these materials to have a pronounced roughness ($R_q > 50$ nm) and the particle size ranging from 0.5 to 2.0 $\mu$m. The atomic force microscopy revealed a change in the surface topography of Fe particles which previous SEM studies failed to detect. Fig. 6 shows that despite a developed relief (peak to peak value, $R_{p-p} = 230$ nm) the major contribution to the change in lateral forces comes from the phase contrast, which allows the phase distribution and the shape of embedded particles to be visualized. The phase contrast variation with the scan rate from 1 to 10 $\mu$m/s is presented in Fig. 3. The curves in this figure demonstrate that the rate

dependence of the lateral contrast increases with increasing surface roughness.

## Conclusion

Thus, the studies performed show that although the surface topography contributes to the lateral image contrast, the main contribution comes from the local chemical composition. For sufficiently smooth surfaces ($R_q < 5$ nm), the surface areas of close crystalline structure with different element concentrations can be well distinguished. For $R_q > 20$ nm LFM investigations make it possible to reveal peculiarities of the relief obtained by AFM studies and to determine the structure of the interfacial regions.

## Acknowledgements

The present work was supported by the RFBR Grants N 00-02-17426 and 01-02-96463.

## References

[1]

[2] H.Gleiter, NanoStuctured Materials, 6 (1995) 3.

[3] V.V.Ivanov, Yu.A.Kotov, A.N.Vikhrev, N.N.Noskova, DAN, 359 (1997) 759, (in Russian).

[4] C.Tien, E.V.Charnaya, V.M.Gropyanov et. al., J. of Mag. and Mag. Mat., 220 (2000) 147.

[5] E.V.Charnaya, N.A.Grigoreva, S.N.Ivanov et al., Phys. Stat. Sol., a147 (1995) 313.

[6] A.V.Antonov, P.A.Arsenev, L.G.Linda et al., Phys. Stat. Sol., a15 (1973) K63. [6] B.Bhushan, S.Sundararajan, Acta. Mater., 46 (1998) 3793.

[7] W.-K. Lee, Polymer, 40 (1999) 5631.